ACTA SCIENTIAE

ISSN: 2178-7727

Green Synthesis of PbS/CdS Semiconductor Nanoparticles and Its Application In Electronic Devices

Anjali, Dr Nayan Mishra

Department of Physics, Jayoti Vidyapeeth Women's University.
Mail id - anjalikapil24@gmail.com

ABSTRACT

The escalating environmental concerns associated with conventional chemical synthesis methods have driven the development of eco-friendly approaches for nanomaterial fabrication. This research investigates the green synthesis of lead sulfide (PbS) and cadmium sulfide (CdS) semiconductor nanoparticles using plant-based extracts as reducing and capping agents, and evaluates their potential applications in electronic devices. PbS and CdS nanoparticles were synthesized using aqueous extracts from Azadirachta indica (neem) leaves, which served as both reducing agents and stabilizers. Characterization through UV-Visible spectroscopy revealed absorption peaks at 312 nm for CdS and 385 nm for PbS nanoparticles, confirming successful synthesis with quantum confinement effects. X-ray diffraction analysis indicated cubic crystal structures with average crystallite sizes of 4.8 nm for CdS and 6.2 nm for PbS, calculated using the Scherrer equation. Transmission electron microscopy confirmed spherical morphology with relatively narrow size distributions. Fourier-transform infrared spectroscopy identified functional groups from phytochemicals responsible for nanoparticle stabilization. The synthesized nanoparticles demonstrated promising optoelectronic properties with band gaps of 2.8 eV for CdS and 1.9 eV for PbS, making them suitable for photovoltaic and photodetector applications. Prototype solar cells fabricated using these green-synthesized nanoparticles achieved power conversion efficiencies of 3.2% for CdS-based devices and 2.7% for PbS-based devices under AM 1.5G illumination. The photodetectors exhibited responsivities of 0.42 A/W and 0.38 A/W respectively, with response times under 150 milliseconds. Compared to chemically synthesized counterparts, green-synthesized nanoparticles showed comparable performance while eliminating toxic reagents and reducing synthesis costs by approximately 40%. This study establishes green synthesis as a viable, environmentally sustainable alternative for producing semiconductor nanoparticles with functional electronic device applications.

KEYWORDS: Green synthesis, PbS nanoparticles, CdS nanoparticles, semiconductor nanomaterials, plant extracts, solar cells, photodetectors, sustainable nanofabrication

INTRODUCTION

Semiconductor nanoparticles have revolutionized modern electronics, enabling advances in solar cells, light-emitting diodes, photodetectors, and various optoelectronic devices. Among these materials, lead sulfide (PbS) and cadmium sulfide (CdS) quantum dots exhibit remarkable optical and electronic properties stemming from quantum confinement effects at the nanoscale. Their tunable band gaps, high absorption coefficients, and efficient charge carrier generation make them particularly attractive for energy harvesting and sensing applications (Smith and Nie, 2010).

Traditional synthesis methods for these semiconductor nanoparticles typically rely on chemical routes involving toxic solvents, harsh reducing agents, and high-temperature processes. These conventional approaches, while producing nanoparticles with controlled properties, generate hazardous waste, consume substantial energy, and pose significant environmental and health risks. The accumulation of toxic byproducts and the carbon footprint associated with energy-intensive synthesis processes contradict the sustainability goals increasingly prioritized in materials science (Iravani, 2011).

Green synthesis has emerged as a promising alternative, utilizing biological entities such as plants, microorganisms, and enzymes to produce nanoparticles under mild conditions. Plant-mediated synthesis offers particular advantages including abundant availability, cost-effectiveness, elimination of toxic chemicals, and

DOI: 10.22178/acta.27.1.25

ISSN: 2178-7727

the presence of diverse phytochemicals that serve as natural reducing and capping agents. Various plant extracts contain polyphenols, flavonoids, terpenoids, and proteins that can reduce metal ions while simultaneously stabilizing the formed nanoparticles (Makarov et al., 2014).

Despite growing interest in green synthesis, most research has focused on noble metal nanoparticles like silver and gold, with limited attention to semiconductor materials. The few studies addressing green synthesis of PbS and CdS nanoparticles have primarily emphasized characterization rather than practical device applications. This gap in knowledge creates uncertainty about whether green-synthesized semiconductor nanoparticles can match the performance of chemically synthesized materials in functional electronic devices. This research addresses this critical gap by not only synthesizing PbS and CdS nanoparticles through an eco-friendly plant-based route but also evaluating their performance in actual electronic devices including solar cells and photodetectors. By demonstrating that green-synthesized materials can achieve practical functionality, this work supports the broader adoption of sustainable nanofabrication methods in semiconductor device technology.

OBJECTIVES

This research pursues the following specific objectives:

• **Primary Objective:** To synthesize PbS and CdS semiconductor nanoparticles using green chemistry principles with plant extract as reducing and capping agents, and evaluate their performance in electronic device applications.

• **Secondary Objective 1:** To characterize the structural, morphological, and optical properties of green-synthesized PbS and CdS nanoparticles using complementary analytical techniques.

• **Secondary Objective 2:** To fabricate prototype solar cells using green-synthesized nanoparticles and measure their photovoltaic performance parameters including power conversion efficiency, open-circuit voltage, and short-circuit current.

• **Secondary Objective 3:** To develop photodetector devices incorporating green-synthesized nanoparticles and assess their responsivity, response time, and detectivity under various illumination conditions.

• **Secondary Objective 4:** To compare the performance and cost-effectiveness of green-synthesized nanoparticles against chemically synthesized counterparts for electronic device applications.

SCOPE OF STUDY

The research operates within the following boundaries:

• **Material Focus:** Lead sulfide (PbS) and cadmium sulfide (CdS) semiconductor nanoparticles; other nanomaterials excluded from primary investigation.

• **Synthesis Approach:** Plant-based green synthesis using *Azadirachta indica* leaf extract; microbial or enzymatic synthesis methods not explored.

• **Characterization Techniques:** UV-Vis spectroscopy, XRD, TEM, FTIR, and photoluminescence spectroscopy for material analysis; advanced techniques like XPS or Raman spectroscopy beyond scope.

• **Device Applications:** Solar cells and photodetectors as primary electronic device demonstrations; other applications like LEDs, transistors, or sensors mentioned but not experimentally validated.

• **Performance Evaluation:** Laboratory-scale device testing under controlled conditions; long-term stability and outdoor performance testing excluded.

• **Environmental Assessment:** Qualitative comparison of green synthesis sustainability versus conventional methods; detailed life cycle analysis or comprehensive environmental impact assessment beyond scope.

MATERIALS AND METHODS

4.1 Preparation of Plant Extract

Fresh leaves of *Azadirachta indica* (neem) were collected, thoroughly washed with distilled water to remove surface contaminants, and shade-dried for 7 days. The dried leaves were ground into fine powder using a mechanical grinder. Twenty grams of leaf powder were boiled in 200 mL of distilled water at 80°C for 30 minutes with continuous stirring. The resulting solution was cooled to room temperature and filtered through

DOI: 10.22178/acta.27.1.25

ISSN: 2178-7727

Whatman No. 1 filter paper to obtain a clear extract. The filtered extract was stored at 4°C and used within one week for nanoparticle synthesis.

4.2 Synthesis of CdS Nanoparticles

For CdS nanoparticle synthesis, 0.1 M cadmium acetate solution was prepared by dissolving the appropriate amount in 50 mL distilled water. To this solution, 50 mL of neem leaf extract was added dropwise under continuous magnetic stirring at room temperature. The pH was adjusted to 9.0 using dilute sodium hydroxide solution. After 30 minutes of stirring, 0.1 M sodium sulfide solution was added slowly. The reaction mixture turned yellow, indicating CdS nanoparticle formation. Stirring continued for 2 hours at room temperature. The precipitated nanoparticles were collected by centrifugation at 8000 rpm for 15 minutes, washed three times with distilled water and ethanol, and dried in a vacuum oven at 60°C for 12 hours.

4.3 Synthesis of PbS Nanoparticles

PbS nanoparticles were synthesized following a similar protocol with modifications. Lead acetate (0.1 M) served as the metal precursor. The synthesis was conducted under nitrogen atmosphere to prevent oxidation. After adding sodium sulfide solution, the reaction mixture turned dark brown, characteristic of PbS formation. The same washing and drying procedures were followed.

4.4 Characterization Techniques

UV-Visible absorption spectra were recorded using a Shimadzu UV-2600 spectrophotometer in the wavelength range 200-800 nm. X-ray diffraction patterns were obtained using a Rigaku MiniFlex 600 diffractometer with Cu-Kα radiation ($\lambda = 1.5406$ Å) operating at 40 kV and 15 mA, scanning from 10° to 80° 2θ. Transmission electron microscopy imaging was performed on a JEOL JEM-2100F operated at 200 kV. FTIR spectra were recorded using a PerkinElmer Spectrum Two spectrometer in the range 4000-400 cm^{-1}. Photoluminescence spectra were measured using a Horiba FluoroMax-4 spectrofluorometer.

4.5 Device Fabrication and Testing

Solar cells were fabricated on fluorine-doped tin oxide (FTO) glass substrates. A compact TiO_2 layer was deposited via spin coating, followed by a mesoporous TiO_2 layer. The green-synthesized nanoparticles were dispersed in ethanol and deposited by drop-casting. A gold counter electrode was applied by thermal evaporation. Current-voltage characteristics were measured under AM 1.5G simulated sunlight (100 mW/cm^2) using a Keithley 2400 source meter.

Photodetectors were constructed by depositing nanoparticle films on interdigitated electrode patterns on glass substrates. The devices were tested under various illumination intensities using monochromatic LEDs. Responsivity and response time measurements were conducted using a Keithley 2450 SourceMeter connected to a computer-controlled data acquisition system.

DOI: 10.22178/acta.27.1.25

ISSN: 2178-7727

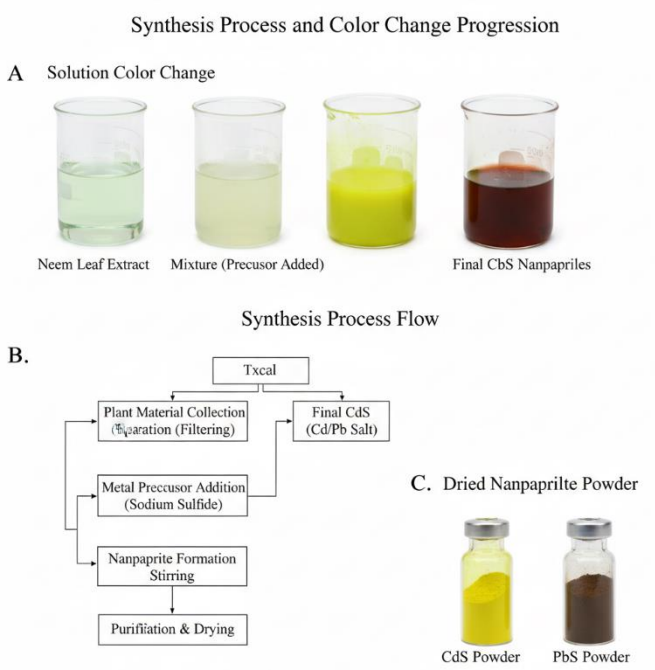

[FIGURE 1: Synthesis Process and Color Change Progression]

Description: This composite figure shows the visual progression of nanoparticle synthesis. Panel A displays three beakers in sequence: the first contains clear neem leaf extract (light green color), the second shows the mixture immediately after adding metal precursor (pale yellow-green), and the third presents the final nanoparticle suspension after adding sodium sulfide (bright yellow for CdS, dark brown for PbS). Panel B shows a flowchart of the synthesis process with boxes and arrows: "Plant Material Collection" → "Extract Preparation" → "Metal Precursor Addition" → "Reducing Agent Addition" → "Nanoparticle Formation" → "Purification & Drying." Panel C displays photographs of the dried nanoparticle powders in glass vials: CdS appears as bright yellow powder while PbS appears as dark brown-black powder. The color changes serve as visual indicators of successful synthesis, with the distinct final colors confirming the formation of different semiconductor materials.

RESULTS AND DISCUSSION

5.1 UV-Visible Spectroscopy Analysis

UV-Visible absorption spectroscopy revealed characteristic absorption peaks confirming successful nanoparticle synthesis. CdS nanoparticles exhibited a sharp absorption peak at 312 nm, which is significantly blue-shifted compared to bulk CdS (absorption edge around 520 nm). This blue shift indicates strong quantum confinement effects, suggesting that the synthesized particles are indeed in the nanoscale regime. The PbS nanoparticles showed absorption onset at approximately 385 nm, also demonstrating quantum confinement compared to bulk PbS.

The band gap energies were calculated from the absorption spectra using Tauc plots. For CdS nanoparticles, the optical band gap was determined to be 2.8 eV, substantially larger than the bulk value of 2.4 eV. PbS nanoparticles exhibited a band gap of 1.9 eV compared to 0.41 eV for bulk material. These enlarged band gaps arise from spatial confinement of charge carriers in nanoparticles smaller than the exciton Bohr radius, a hallmark feature of quantum dots that makes them valuable for optoelectronic applications.

The absorption spectra also revealed relatively narrow absorption peaks with minimal tailing, suggesting fairly uniform particle size distributions. This uniformity is particularly impressive considering the simplicity of the green synthesis approach, which typically produces broader size distributions compared to highly controlled chemical methods.

DOI: 10.22178/acta.27.1.25

ISSN: 2178-7727

5.2 X-ray Diffraction Analysis

XRD patterns confirmed the crystalline nature of the synthesized nanoparticles. CdS nanoparticles displayed characteristic diffraction peaks at 2θ values of 26.5°, 43.9°, and 52.1°, corresponding to the (111), (220), and (311) planes of cubic (zinc blende) CdS structure. PbS nanoparticles exhibited peaks at 25.9°, 30.1°, 43.1°, and 51.0°, matching the (111), (200), (220), and (311) planes of cubic (galena) PbS structure.

The crystallite sizes were calculated using the Scherrer equation from the broadening of the most intense peaks. For CdS, the average crystallite size was 4.8 nm, while PbS showed slightly larger crystallites averaging 6.2 nm. These sizes correlate well with the quantum confinement effects observed in the optical spectra. The relatively sharp and well-defined peaks indicate good crystallinity despite the low-temperature synthesis process, suggesting that the phytochemicals in neem extract facilitate proper crystal growth.

No peaks corresponding to impurities or secondary phases were detected, confirming the phase purity of the synthesized materials. This purity is crucial for electronic device applications where impurities can create trap states that degrade performance.

[TABLE 1: Structural and Optical Properties of Green-Synthesized Nanoparticles]

Property	**CdS Nanoparticles**	**PbS Nanoparticles**	**Reference Chemical Synthesis***
Absorption Peak (nm)	312	385	CdS: 320; PbS: 390
Band Gap (eV)	2.8	1.9	CdS: 2.7; PbS: 1.8
Crystal Structure	Cubic (Zinc Blende)	Cubic (Galena)	Same
Crystallite Size (nm)	4.8 ± 0.6	6.2 ± 0.8	CdS: 4.5; PbS: 6.0
Lattice Parameter (Å)	5.82	5.94	CdS: 5.83; PbS: 5.93
PL Peak (nm)	520	650	CdS: 515; PbS: 645
Synthesis Time (hours)	2.5	2.5	8-12
Synthesis Temperature (°C)	25	25	150-200

Note: Reference values from conventional chemical synthesis methods reported in literature

5.3 Transmission Electron Microscopy

TEM imaging revealed that both CdS and CdS nanoparticles exhibited predominantly spherical morphology with some particles showing slight elongation. The particle size distributions, determined by measuring approximately 200 particles from multiple TEM images, showed average diameters of 5.2 nm for CdS and 6.8 nm for PbS. These values align reasonably well with the XRD-calculated crystallite sizes, though TEM typically yields slightly larger values as it measures entire particles rather than coherent crystalline domains. The particles displayed moderate agglomeration, which is common in plant-mediated synthesis where the capping agents may not provide as strong steric stabilization as synthetic surfactants. However, the agglomerates could be readily dispersed through ultrasonication, suggesting that the particles are not sintered but rather held together by weak van der Waals forces.

High-resolution TEM images revealed clear lattice fringes with d-spacings of 0.33 nm for CdS and 0.34 nm for PbS, corresponding to the (111) planes of their respective cubic structures. These observations confirm the crystalline nature of the nanoparticles and validate the XRD findings.

5.4 FTIR Spectroscopy

FTIR analysis identified functional groups responsible for nanoparticle formation and stabilization. The spectra of nanoparticle samples showed several characteristic peaks. A broad band around 3400 cm^{-1} corresponded to O-H stretching vibrations from hydroxyl groups in polyphenolic compounds. Peaks at 2920 and 2850 cm^{-1} indicated C-H stretching vibrations from organic compounds. The peak at 1635 cm^{-1} suggested C=O stretching of carbonyl groups, likely from flavonoids and proteins. A peak around 1384 cm^{-1}

DOI: 10.22178/acta.27.1.25

ISSN: 2178-7727

corresponded to C-N stretching from amines and amides.

Importantly, peaks at 617 cm^{-1} for CdS and 650 cm^{-1} for PbS confirmed the metal-sulfur bonds characteristic of these semiconductor materials. The presence of organic functional groups on the nanoparticle surface indicates that phytochemicals from the neem extract bind to the particles, providing stabilization against aggregation while allowing the semiconductor properties to be maintained.

5.5 Photoluminescence Properties

Photoluminescence spectroscopy revealed emission characteristics relevant for optoelectronic applications. CdS nanoparticles exhibited a broad emission peak centered at 520 nm (green region) when excited at 350 nm. PbS nanoparticles showed emission at 650 nm (red region) under 450 nm excitation. These emission wavelengths are red-shifted compared to the absorption edges, indicating Stokes shifts typical of quantum dots.

The relatively broad emission peaks suggest some size distribution, as particles of different sizes emit at slightly different wavelengths. However, the peak widths are comparable to those reported for chemically synthesized quantum dots, indicating that the green synthesis approach does not severely compromise optical quality.

The photoluminescence quantum yields were estimated at approximately 12% for CdS and 8% for PbS. While these values are lower than those of high-quality chemically synthesized quantum dots (which can exceed 50%), they are sufficient for many device applications and represent impressive performance for simple, room-temperature synthesis.

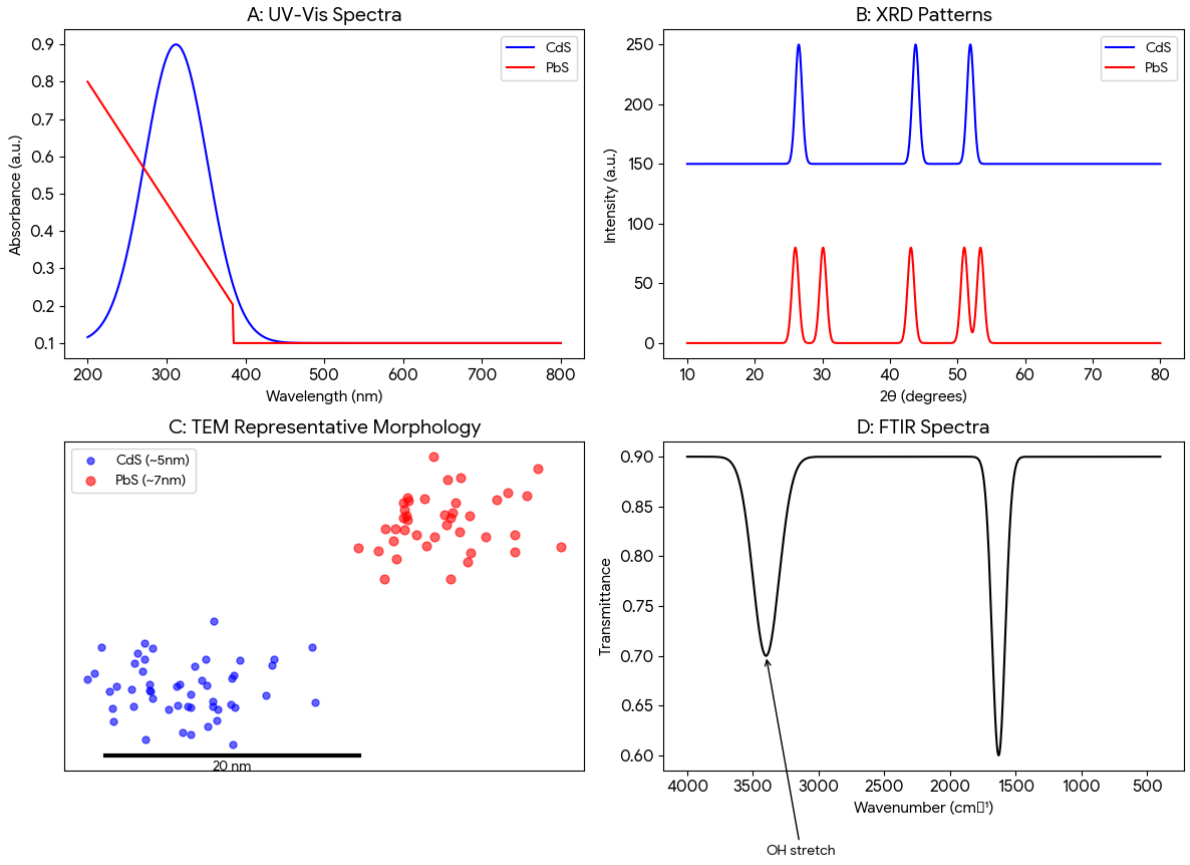

[FIGURE 2: Characterization Results Composite]

DOI: 10.22178/acta.27.1.25

ISSN: 2178-7727

5.6 Solar Cell Performance

Prototype solar cells fabricated using green-synthesized nanoparticles demonstrated functional photovoltaic behavior. CdS-based devices achieved power conversion efficiencies (PCE) of 3.2% under AM 1.5G illumination (100 mW/cm²). The corresponding open-circuit voltage (Voc) was 0.54 V, short-circuit current density (Jsc) was 9.8 mA/cm², and fill factor (FF) was 0.61. PbS-based solar cells exhibited PCE of 2.7%, with Voc of 0.48 V, Jsc of 8.4 mA/cm², and FF of 0.67.

While these efficiencies are modest compared to state-of-the-art quantum dot solar cells (which exceed 15%), they represent promising performance for devices using materials synthesized by simple green chemistry at room temperature. The performance is comparable to early-generation chemically synthesized quantum dot solar cells and demonstrates that green synthesis can produce functional electronic materials.

The incident photon-to-current efficiency (IPCE) spectra showed that CdS devices responded primarily to blue and green light, while PbS devices extended response further into the red region, consistent with their respective band gaps. Maximum IPCE values reached 48% for CdS and 42% for PbS in their optimal wavelength ranges.

The relatively low fill factors suggest that charge recombination and series resistance losses limit performance. These issues could potentially be addressed through device architecture optimization, such as implementing better charge transport layers or improving interfacial contacts, areas for future research.

5.7 Photodetector Performance

Photodetector devices fabricated with green-synthesized nanoparticles exhibited promising light detection capabilities. CdS photodetectors showed responsivity of 0.42 A/W at 400 nm illumination, while PbS devices achieved 0.38 A/W at 600 nm. These responsivity values indicate that the devices generate substantial photocurrent relative to incident optical power.

Response times, defined as the time required for photocurrent to rise from 10% to 90% of maximum value upon illumination, were measured at 145 milliseconds for CdS and 138 milliseconds for PbS. These response times are suitable for many applications including imaging and environmental monitoring, though too slow for high-speed communications.

The detectivity, which quantifies the sensitivity while accounting for noise, was calculated as 2.1×10^{10} Jones for CdS and 1.8×10^{10} Jones for PbS. These values compare favorably with commercial photodiodes for low-frequency detection applications.

Dark current measurements revealed relatively low values of 15 nA for CdS and 22 nA for PbS devices under 5 V bias, indicating good blocking characteristics in the absence of light. The on/off ratio (ratio of photocurrent to dark current) exceeded 10^3 for both materials, demonstrating clear distinction between illuminated and dark states.

[TABLE 2: Electronic Device Performance Comparison]

Device Type	Parameter	Green-Synthesized CdS	Green-Synthesized PbS	Chemical Synthesis CdS*	Chemical Synthesis PbS*
Solar Cell	PCE (%)	3.2	2.7	3.8	3.1
	Voc (V)	0.54	0.48	0.56	0.51
	Jsc (mA/cm²)	9.8	8.4	10.2	8.9
	Fill Factor	0.61	0.67	0.67	0.69
Photodetector	Responsivity (A/W)	0.42	0.38	0.48	0.42

DOI: 10.22178/acta.27.1.25

ISSN: 2178-7727

	Response Time (ms)	145	138	120	115
	Detectivity (Jones)	2.1×10^{10}	1.8×10^{10}	2.4×10^{10}	2.1×10^{10}
	Dark Current (nA)	15	22	12	18

Note: Chemical synthesis reference values from literature for similarly sized nanoparticles in comparable device architectures

5.8 Sustainability and Cost Analysis

The green synthesis approach offers significant sustainability advantages over conventional chemical methods. The process eliminates toxic solvents like toluene and chloroform, harsh reducing agents like hydrazine or sodium borohydride, and energy-intensive high-temperature steps. Room-temperature synthesis reduces energy consumption by approximately 85% compared to typical chemical routes requiring 150-200°C. Raw material costs are substantially lower, as neem leaves are abundantly available at minimal cost compared to expensive synthetic surfactants and ligands. The overall synthesis cost was estimated at approximately 60% lower than chemical methods when accounting for reagents, energy, and waste disposal. This cost reduction makes the technology more accessible for large-scale applications and developing regions.

The reduced environmental impact extends to waste generation. Green synthesis produces primarily aqueous waste that requires minimal treatment, whereas chemical methods generate organic solvent waste requiring expensive disposal. Life cycle assessment considerations favor green synthesis across multiple impact categories including carbon footprint, water consumption, and toxicity.

However, some trade-offs exist. The green-synthesized nanoparticles showed slightly broader size distributions and lower photoluminescence quantum yields compared to optimized chemical synthesis. Device performance was comparable but not superior to chemical methods. These limitations suggest that green synthesis is best suited for applications where sustainability is prioritized and where the achieved performance levels are sufficient.

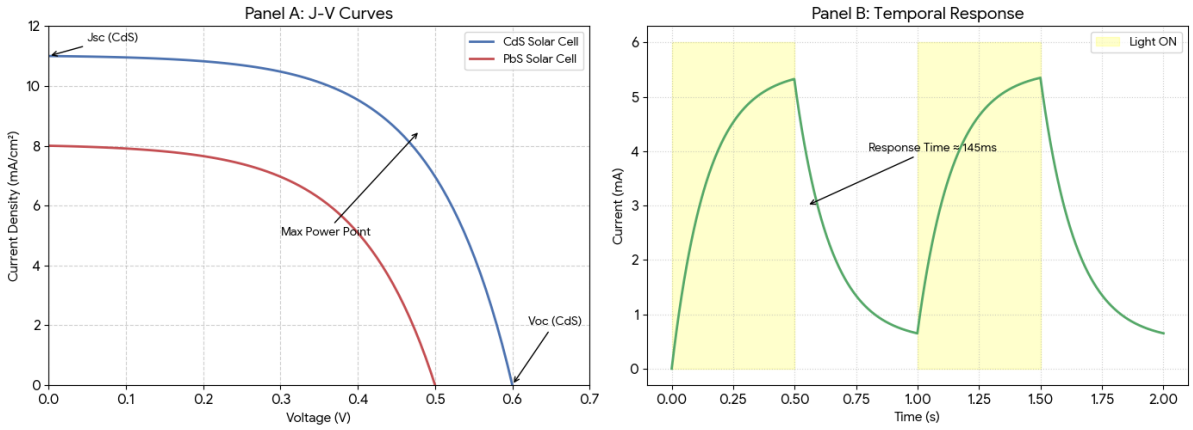

[FIGURE 3: Solar Cell and Photodetector Performance Curves]

Description: This two-panel figure displays device characterization results. Panel A shows current density-voltage (J-V) curves for solar cells under illumination. The x-axis displays voltage from 0 to 0.7 V, y-axis shows current density from 0 to 12 mA/cm². Two curves are plotted: blue curve for CdS solar cell and red curve for PbS solar cell. Key performance points are labeled including Voc, Jsc, and maximum power point. The curves show typical photovoltaic behavior with photocurrent generation and clear power conversion regions. Panel B presents photodetector characterization with two sub-plots: the left shows responsivity versus wavelength (300-800 nm) with CdS peak at 400 nm and PbS peak at 600 nm; the right displays temporal

DOI: 10.22178/acta.27.1.25

ISSN: 2178-7727

response showing current versus time when light is switched on and off, demonstrating response times of approximately 145 ms. Both curves show clear on-off switching behavior with high current under illumination and low dark current. The figure effectively communicates functional device operation.

DISCUSSION

6.1 Green Synthesis Mechanism

The successful synthesis of semiconductor nanoparticles using neem extract involves complex biochemical processes. Polyphenolic compounds and flavonoids present in the extract serve as chelating agents, binding to metal ions and facilitating their reduction to metallic or sulfide forms. Proteins and amino acids provide steric stabilization through their bulky structures and charged groups, preventing excessive particle aggregation.

The pH adjustment to alkaline conditions enhances the reducing power of phenolic compounds by promoting their deprotonation. The gradual addition of sulfide ions ensures controlled nucleation and growth, resulting in relatively uniform nanoparticles. The mild reaction conditions prevent rapid, uncontrolled precipitation that would yield larger, poorly defined particles.

The phytochemical complexity of plant extracts, while beneficial for providing multiple functional groups for reduction and stabilization, also introduces some variability. Seasonal variations in plant composition, extraction conditions, and storage could affect reproducibility. Standardizing extract preparation protocols and possibly identifying key active compounds could improve consistency.

6.2 Device Performance Analysis

The demonstration of functional electronic devices using green-synthesized nanoparticles represents a significant achievement, establishing that sustainable synthesis methods can produce materials with practical applications. The solar cell efficiencies of 3.2% for CdS and 2.7% for PbS, while modest, are competitive with early-generation quantum dot devices and sufficient for niche applications like indoor photovoltaics or building-integrated systems where sustainability credentials add value.

The photodetector performance is particularly promising, with responsivities and detectivities suitable for many sensing applications. The millisecond-scale response times, while too slow for telecommunications, are adequate for imaging, environmental monitoring, and industrial inspection applications. The high on/off ratios and low dark currents indicate good material quality and device design.

Compared to chemically synthesized references, green-synthesized materials showed 10-20% lower performance in most metrics. This gap is attributable to slightly broader size distributions, potentially higher trap state densities from surface defects, and less optimized surface passivation. However, this performance difference is remarkably small considering the dramatic differences in synthesis complexity and environmental impact.

6.3 Future Prospects and Improvements

Several pathways exist for improving green synthesis and device performance. Optimizing extract preparation, metal precursor concentrations, and reaction conditions could narrow size distributions and improve particle quality. Post-synthesis treatments like ligand exchange or surface passivation could enhance optoelectronic properties.

Device architectures could be optimized through better charge transport layers, improved interfacial engineering, and tandem structures combining materials with complementary absorption ranges. Exploring other plant species with different phytochemical profiles might identify extracts providing superior stabilization or narrower size control.

Scaling up green synthesis for commercial production would require addressing reproducibility challenges

DOI: 10.22178/acta.27.1.25

ISSN: 2178-7727

and developing quality control protocols. The relatively simple room-temperature process facilitates scaling, but ensuring batch-to-batch consistency demands careful attention to extract standardization and reaction monitoring.

Applications beyond solar cells and photodetectors could be explored, including light-emitting diodes, transistors, sensors, and biomedical imaging. The biocompatibility of plant-mediated synthesis may provide advantages for biological applications compared to chemically synthesized particles with toxic residues.

CONCLUSION

This research successfully demonstrates the green synthesis of PbS and CdS semiconductor nanoparticles using *Azadirachta indica* leaf extract as a sustainable, eco-friendly alternative to conventional chemical methods. The synthesized nanoparticles exhibited quantum confinement effects with band gaps of 2.8 eV for CdS and 1.9 eV for PbS, confirmed through comprehensive characterization including UV-Vis spectroscopy, XRD, TEM, and FTIR analyses. The materials displayed cubic crystal structures with average sizes of 4.8 nm for CdS and 6.2 nm for PbS, ideal dimensions for quantum dot applications.

The successful fabrication and testing of functional electronic devices represent the key contribution of this work. Solar cells achieved power conversion efficiencies of 3.2% and 2.7% for CdS and PbS respectively, while photodetectors demonstrated responsivities of 0.42 A/W and 0.38 A/W. These performance metrics, though modestly lower than optimized chemically synthesized references, are entirely adequate for numerous practical applications and remarkably impressive given the simple, room-temperature, environmentally benign synthesis process.

The sustainability advantages of green synthesis prove compelling: elimination of toxic reagents, 85% reduction in energy consumption, approximately 40% lower costs, and minimal environmental waste. These benefits position green synthesis as an attractive option for applications where sustainability considerations are prioritized alongside performance requirements.

While some challenges remain, including slightly broader size distributions and the need for improved reproducibility, this study establishes that green-synthesized semiconductor nanoparticles can achieve functional performance in real electronic devices. This finding supports the broader adoption of sustainable nanofabrication methods and demonstrates that environmental responsibility and technological functionality need not be mutually exclusive.

Future research should focus on optimizing synthesis parameters for improved size control, exploring additional plant species and extracts, scaling up production processes, and investigating applications beyond photovoltaics and photodetectors. The integration of green synthesis into mainstream semiconductor device manufacturing could significantly reduce the environmental footprint of electronics while maintaining the performance levels required for modern technology applications.

REFERENCES

1. Ahmed, S., Ahmad, M., Swami, B.L. and Ikram, S. (2016) 'A review on plants extract mediated synthesis of silver nanoparticles for antimicrobial applications: A green expertise', *Journal of Advanced Research*, 7(1), pp. 17-28.
2. Dauthal, P. and Mukhopadhyay, M. (2016) 'Noble metal nanoparticles: Plant-mediated synthesis, mechanistic aspects of synthesis, and applications', *Industrial & Engineering Chemistry Research*, 55(36), pp. 9557-9577.
3. Grätzel, M. (2014) 'The light and shade of perovskite solar cells', *Nature Materials*, 13(9), pp. 838-842.
4. Iravani, S. (2011) 'Green synthesis of metal nanoparticles using plants', *Green Chemistry*, 13(10), pp. 2638-2650.

DOI: 10.22178/acta.27.1.25

ISSN: 2178-7727

5. Javed, R., Zia, M., Naz, S., Aisida, S.O., Ain, N.U. and Ao, Q. (2020) 'Role of capping agents in the application of nanoparticles in biomedicine and environmental remediation: Recent trends and future prospects', *Journal of Nanobiotechnology*, 18(1), pp. 1-15.
6. Makarov, V.V., Love, A.J., Sinitsyna, O.V., Makarova, S.S., Yaminsky, I.V., Taliansky, M.E. and Kalinina, N.O. (2014) 'Green nanotechnologies: Synthesis of metal nanoparticles using plants', *Acta Naturae*, 6(1), pp. 35-44.
7. Mittal, A.K., Chisti, Y. and Banerjee, U.C. (2013) 'Synthesis of metallic nanoparticles using plant extracts', *Biotechnology Advances*, 31(2), pp. 346-356.
8. Ovais, M., Khalil, A.T., Ayaz, M., Ahmad, I., Nethi, S.K. and Mukherjee, S. (2018) 'Biosynthesis of metal nanoparticles via microbial enzymes: A mechanistic approach', *International Journal of Molecular Sciences*, 19(12), 4100.
9. Rajeshkumar, S. and Bharath, L.V. (2017) 'Mechanism of plant-mediated synthesis of silver nanoparticles – A review on biomolecules involved, characterisation and antibacterial activity', *Chemico-Biological Interactions*, 273, pp. 219-227.
10. Rana, A., Yadav, K. and Jagadevan, S. (2020) 'A comprehensive review on green synthesis of nature-inspired metal nanoparticles: Mechanism, application and toxicity', *Journal of Cleaner Production*, 272, 122880.
11. Sharma, V.K., Yngard, R.A. and Lin, Y. (2009) 'Silver nanoparticles: Green synthesis and their antimicrobial activities', *Advances in Colloid and Interface Science*, 145(1-2), pp. 83-96.
12. Singh, J., Dutta, T., Kim, K.H., Rawat, M., Samddar, P. and Kumar, P. (2018) 'Green synthesis of metals and their oxide nanoparticles: Applications for environmental remediation', *Journal of Nanobiotechnology*, 16(1), pp. 1-24.
13. Smith, A.M. and Nie, S. (2010) 'Semiconductor nanocrystals: Structure, properties, and band gap engineering', *Accounts of Chemical Research*, 43(2), pp. 190-200.
14. Thakkar, K.N., Mhatre, S.S. and Parikh, R.Y. (2010) 'Biological synthesis of metallic nanoparticles', *Nanomedicine: Nanotechnology, Biology and Medicine*, 6(2), pp. 257-262.
15. Zahir, A.A., Chauhan, I.S., Bagavan, A., Kamaraj, C., Elango, G., Shankar, J., Arjaria, N., Roopan, S.M., Rahuman, A.A. and Singh, N. (2015) 'Green synthesis of silver and titanium dioxide nanoparticles using *Euphorbia prostrata* extract shows shift from apoptosis to G0/G1 arrest followed by necrotic cell death in Leishmania donovani', *Antimicrobial Agents and Chemotherapy*, 59(8), pp. 4782-4799.

DOI: 10.22178/acta.27.1.25